Pharmacol Toxicol Nat Med 2026, 6(1): 1-14
DOI: 10.52406/ptnm.v6i1.141

Doxorubicin-induced Hepatorenal Dysfunctions in Wistar rats: Mechanistic Protective Role of Diosmin-Hesperidin Fixed-Dose Combinations Mediated via Oxidative and Inflammatory Stress Suppression

Adejuwon A. Adeneye[1,2*], Kehinde S. Fashikun[1], Nadrah G. Akinlade[1], Abdulfatai O. Ojewale[3], Ikechuckwu I. Okoye[4]

[1]Department of Pharmacology, Therapeutics and Toxicology, Faculty of Basic Clinical Sciences, Lagos State University College of Medicine, 1-5 Oba Akinjobi Way, G.R.A., Ikeja, Lagos State, Nigeria. [2]Directorate of Research Management and Innovation, Office of the Vice Chancellor, 3rd Floor, Babatunde Raji Fashola Senate Building, Main Campus, Lagos State University, Ojo, Lagos State, Nigeria. [3]Department of Anatomy, Faculty of Basic Medical Sciences, Lagos State University College of Medicine, 1-5 Oba Akinjobi Way, G.R.A., Ikeja, Lagos State, Nigeria. [4]Department of Pathology and Oral Medicine, Faculty of Dentistry, Lagos State University College of Medicine, 1-5 Oba Akinjobi Way, G.R.A., Ikeja, Lagos State, Nigeria.

***Corresponding Author:** adejuwon.adeneye@lasucom.edu.ng* ***Phone:** +2348035835589*

ARTICLE HISTORY
Received: 16th November, 2025
Accepted: 24th December, 2025

KEYWORDS
Diosmin-Hesperidin combination, Doxorubicin, Hepatorenal toxicity, Oxidative stress, Inflammation

Pharmacology and Toxicology of Natural Medicines ISSN: 2756-6838

Published by ***Phytomedicine Research Group,*** *Department of Pharmacology & Toxicology, Faculty of Pharmacy, University of Benin, Benin City 300001, Nigeria*

ABSTRACT

Background and Purpose: Doxorubicin (DOX), a widely used chemotherapeutic agent, is associated with severe off target hepatorenal toxicity due to oxidative stress, inflammation and apoptosis. This study investigated the possible protective effects of 50-200 mg/kg/day pretreatment of a fixed-dose combination of diosmin-hesperidin (DH) against DOX-induced hepatorenal toxicity in male Wistar rats.

Methods: Forty-eight (48) young adult male Wistar rats were randomly allotted to 8 treatment groups of 6 rats per group and orally pretreated with DH at doses of 50, 100, and 200 mg/kg/day as well as 20 mg/kg/day silymarin (SIL), before DOX administration (3 mg/kg/i.p. route on alternate days), all for 10 days. Hepatic and renal function tests, oxidative stress markers [superoxide dismutase (SOD), catalase (CAT), malondialdehyde (MDA), and reduced glutathione (GSH)], inflammatory markers [tumor necrosis factor-alpha (TNF-α) and interleukin-10 (IL-10)], and histopathological assessments were the measuring endpoints.

Results: Biochemical analysis revealed that repeated treatment with DOX significantly ($P<0.05$, $P<0.001$, and $P<0.0001$) impaired hepatic and renal function, increased oxidative stress (elevated MDA, reduced SOD, CAT, and GSH), and promoted inflammation (elevated TNF-α and reduced IL-10). Histopathological analysis revealed severe hepatic and tubulo-glomerular degenerative changes. DH pretreatment effectively mitigated DOX-induced toxicity by improving hepatic and renal function, restoring oxidative balance, reducing inflammation, and preserving tissue architecture in a dose-dependent manner. The highest dose (200 mg/kg) provided the most significant hepatoprotective and renoprotective effects.

Conclusion: These findings suggest that DH exerts protective effects against DOX-induced hepatorenal toxicity through its antioxidant and anti-inflammatory properties. This study highlights the therapeutic potential of DH as an adjunct in chemotherapy-induced organ toxicity.

INTRODUCTION

Doxorubicin (DOX) is a widely used anthracycline antibiotic employed in cancer chemotherapy due to its broad-spectrum antineoplastic activity (Puna *et al.*, 2017; D'Angelo *et al.*, 2022). Although the precise cytotoxic mechanisms of DOX are poorly understood, emerging evidence suggests that its pleiotropic anticancer activity include its contribution to DNA cleavage, reactive oxygen species (ROS) generation, induction of apoptosis, senescence, autophagy, ferroptosis, and pyroptosis, as well as its immunomodulatory role (Kciuk *et al.*, 2023). DOX slows cancer growth by binding to and inhibiting the activity of topoisomerase II enzyme, which regulates cancer cell growth and division and consequently causing DNA damage and induction of apoptosis (Johnson-Arbor and Dubey, 2025). However, its clinical utility is significantly limited by its severe adverse effects, particularly hepatotoxicity and nephrotoxicity (Guo *et al.*, 2016; Afsar *et al.*, 2020; Alherz *et al.*, 2023; Qaed *et al.*, 2024). These toxic effects are largely attributed to increased oxidative stress, inflammation, and mitochondrial dysfunction, leading to tissue damage. The liver and kidneys, being major organs involved in drug metabolism and excretion, are highly susceptible to DOX-induced toxicity, which manifests as elevated biomarkers of organ dysfunction, oxidative stress, and inflammatory responses (Guo *et al.*, 2016; Owumi *et al.*, 2021; Saleh *et al.*, 2022). Given these deleterious effects, the need for protective strategies against DOX-induced hepatorenal toxicity is critical.

Flavonoids, particularly diosmin and hesperidin, have garnered significant interest for their potent anticancer activities which are primarily mediated by inducing apoptosis via caspase activation and DNA damage, halting cell proliferation by arresting the cell cycle (S-phase), downregulating growth markers like Ki67, inhibiting angiogenesis/metastasis by blocking pathways like NF-κB and Wnt/STAT, reducing inflammation (TNF-α, COX-2), and slowing tumor growth (Aggarwal *et al.*, 2020; Rahman *et al.*, 2024; Faezi *et al.*, 2025). They are also known to possess neuroprotective, cardioprotective, antioxidant, anti-inflammatory, and cytoprotective properties (Ullah *et al.*, 2020; Huwait and Mobashir, 2022). Diosmin, a naturally occurring flavone glycoside, and hesperidin, a flavanone glycoside, have demonstrated protective effects against various forms of organ toxicity by scavenging free radicals, enhancing endogenous antioxidant defense mechanisms, and modulating inflammatory responses. Their combination has been widely used in vascular disorders and holds promise for mitigating chemotherapy-induced toxicity (Gerges *et al.*, 2022; Huwait and Mobashir, 2022).

This study aims to evaluate the protective effects of a fixed-dose combination of diosmin and hesperidin (DH) against DOX-induced hepatorenal toxicity in male Wistar rats. Specifically, the study seeks to assess hepatic and renal function through biochemical markers; evaluate oxidative stress markers, including superoxide dismutase (SOD), catalase (CAT), malondialdehyde (MDA), and reduced glutathione (GSH), in hepatic and renal tissues; determine inflammatory responses by measuring tumor necrosis factor-alpha (TNF-α) and interleukin-10 (IL-10) levels; and conduct histopathological examinations of hepatic and renal tissues to assess structural integrity and cellular damage.

Despite the efficacy of DOX in cancer treatment, its dose-dependent toxicity to non-cancerous tissues remains a major concern (Lee *et al.*, 2023). Conventional approaches to mitigating its adverse effects, such as co-administration of synthetic antioxidants, have shown limited success and may present additional side effects (Petcu *et al.*, 2023). Natural compounds with established safety profiles and potent antioxidative and anti-inflammatory properties offer an alternative therapeutic strategy (Pradubyat *et al.*, 2024).

Diosmin and hesperidin have been extensively studied for their vascular protective effects (Gölboyu *et al.*, 2024), yet their role in protecting against DOX-induced hepatorenal toxicity remains underexplored. Their combined administration has been shown to enhance bioavailability and synergistically exert stronger antioxidant and anti-inflammatory effects than when used individually (Carballo-Villalobos *et al.*, 2016; Huwait and Mobashir, 2022). By evaluating their hepatoprotective and renoprotective efficacy in an experimental DOX-induced toxicity model, this study may provide valuable insights into their potential as adjuvant therapy in chemotherapy-induced organ damage. Furthermore, this study utilizes a comprehensive approach by assessing biochemical, oxidative stress, inflammatory, and histopathological parameters, ensuring a holistic understanding of DH's protective mechanisms. Thus, findings from this research may contribute to developing novel therapeutic interventions to improve patient outcomes during chemotherapy while minimizing organ damage.

MATERIALS AND METHODS

Experimental Animals

Young male Wistar Albino rats (aged 6–8 weeks, weighing 90–125 g) were procured from Bayo Farms, Sango-Ota, Ogun State, following ethical approval (with the reference number: LASU/23/REC/083) from the Lagos State University Research Ethics Committee, Lagos State University, Ojo, Nigeria. Upon arrival, the rats were housed in the Lagos State University College of Medicine (LASUCOM) Animal House, where they underwent a two-week acclimatization period. Throughout the period, they were cared for in accordance with international best

practices for the handling and use of laboratory animals, as outlined by ARRIVE guidelines (Percie du Sert *et al.*, 2020) and the National Research Council (US) Committee for the Update of the Guide for the Care and Use of Laboratory Animals (2011). The rats had unrestricted access to standard rat chow and potable tap water and were maintained under optimal laboratory conditions for the duration of the study.

After acclimatization, the rats were randomly assigned to eight (8) treatment groups consisting of six (6) rats per group, ensuring that intra- and inter-group weight variations did not exceed ±20% of the average weight of the sample population.

Body Weight Measurement and Calculation of Percentage Weight Change (%Δwt)

Body weights were recorded at both the start and conclusion of the experiment using a digital rodent weighing scale (Virgo Electronic Compact Scale®, New Delhi, India). All measurements were expressed in grams (g). The percentage weight change (%Δwt) was determined using the formula earlier described by Adeneye *et al.* (2024).

Induction of DOX-Induced Hepatorenal Toxicity and Treatment Protocol

Doxorubicin (DOX)-induced hepatorenal toxicity was established using a modified method by Adeneye *et al.* (2021). The rats were randomly allotted to eight groups (n = 5 per group), ensuring that weight differences remained within ±20% of the average sample population weight.

Treatment regimens for each group are outlined in Table 1. Experimental rats were pre-treated orally for 10 days with either sterile water (10 mL/kg/day), Daflon® (90% diosmin-10% hesperidin fixed-dose combination, 50-200 mg/kg/day; Daflon-1000 mg®, Les Laboratoires Servier Industrie, France), or silymarin (20 mg/kg/day; Silyborn-140®, Micro Labs Limited, India) before receiving an intraperitoneal injection of DOX (3 mg/kg/day) as a single dose on alternate days for 10 days. Drug dosages were determined based on preliminary dose-finding studies.

Table 1: Treatment protocol.

Groups	Treatments
I	10 mL/kg/day of sterile water given *p.o.* daily for 10 consecutive days + 1 mL/kg/day of sterile water given *i.p.* 1 h after sterile water (SW) treatment on alternate days for 10 days.
II	10 mL/kg/day sterile water (SW) given *p.o.* daily for 10 consecutive days + 3 mg/kg/day DOX in sterile water given *i.p.* as a single bolus 1 h after sterile water (SW) treatment on alternate days for 10 days.
III	200 mg/kg/day 90% diosmin-10% hesperidin fixed dose combination in sterile water (DH) given *p.o.* daily for 10 consecutive days + 1 mL/kg/day sterile water given *i.p.* 1 h after 90% diosmin-10% hesperidin fixed dose combination (DH) treatment for 10 days.
IV	50 mg/kg/day 90% diosmin-10% hesperidin fixed dose combination in sterile water (DH) given *p.o.* daily for 10 consecutive days + 3 mg/kg/day DOX in sterile water given *i.p.* as a single bolus 1 h after 90% diosmin-10% hesperidin fixed dose combination (DH) treatment on alternate days for 10 days
V	100 mg/kg/day 90% diosmin-10% hesperidin fixed dose combination in sterile water (DH) given *p.o.* daily for 10 consecutive days + 3 mg/kg/day DOX in sterile water given *i.p.* as a single bolus 1 h after the last dose of metformin
VI	200 mg/kg/day metformin in sterile water given *p.o.* daily for 10 consecutive days + 3 mg/kg/day DOX in sterile water given *i.p.* as a single bolus 1 h after 90% diosmin-10% hesperidin fixed dose combination (DH) treatment for 10 days
VII	20 mg/kg/day silymarin (SIL) in sterile water given *p.o.* daily for 10 days + 1 mL/kg/day of sterile water given *i.p.* as a single bolus 1 h after sterile water treatment on alternate days for 10 days
VIII	20 mg/kg/day silymarin in distilled water (SIL) given *p.o.* daily for 10 days + 3 mg/kg/day DOX given *i.p.* 1 h after silymarin treatment on alternate days for 10 days

Blood and Tissue Sample Collection

Twenty-four hours after the final DOX administration, the rats were fasted overnight and euthanized with light inhalational halothane. Whole blood samples were collected directly from the heart using a 21G needle and a 5 mL syringe, ensuring minimal tissue damage. Subsequently, a midline surgical incision was performed to expose and carefully excise the liver. The blood samples were collected into plain bottles and allowed to clot at room temperature for 1 h. Following euthanasia, carcasses were properly processed and disposed of by trained and certified Animal House Attendants in compliance with established

protocols for the safe disposal of medical and toxic waste, including deceased experimental animals (Adeneye *et al.*, 2021; 2024; Olorundare *et al.*, 2024).

Hepatic and Renal Function Assessments

Serum samples were obtained by centrifuging the clotted blood at 2000 x *g* for 10 min in a refrigerated centrifuge. The clear yellow (straw-color) supernatants obtained were transferred into new, clean tubes, using a pipette. The sera were analyzed for hepatic function markers, including alanine aminotransferase (ALT), aspartate aminotransferase (AST), alkaline phosphatase (ALP), total protein (TP), albumin (ALB), and total bilirubin (TB). Renal function parameters assessed included serum electrolytes [sodium (Na^+), potassium (K^+), and chloride (Cl^-)], blood urea nitrogen (BUN), and creatinine (Cr). All assays were performed using standard bioassay protocols and commercially available diagnostic kits (Randox Diagnostics Test Kits®, Randox Laboratories Ltd., UK), following the manufacturer's instructions and previous methodologies by Adeneye *et al.* (2021).

Hepatic and Renal Tissue Antioxidant Enzyme Assays

Markers of oxidative stress, including glutathione (GSH), malondialdehyde (MDA), catalase (CAT), and superoxide dismutase (SOD), were quantified using methods previously described by Adeneye *et al.* (2024) and Olorundare *et al.* (2024).

Quantification of TNF-α and IL-10 in Hepatic and Renal Tissues

Hepatic and renal tissue levels of tumor necrosis factor-alpha (TNF-α) and interleukin-10 (IL-10) were determined using enzyme-linked immunosorbent assay (ELISA) kits {Quantikine Rat TNF-α (RTA00-1) and IL-10 (PT1000); R&D Systems Inc., USA}. The procedures followed the manufacturer's guidelines, with results expressed in picograms per milliliter (pg/mL).

Histopathological Examination of Hepatic and Renal Tissues

Tissue sections from the liver and kidneys were prepared, stained with hematoxylin and eosin, and analyzed following the histopathological protocols outlined by Adeneye *et al.* (2021; 2024).

Data Analysis

Data are presented as mean ± standard deviation (SD) for body weight measurements and mean ± standard error of the mean (SEM) for biochemical analyses. Statistical comparisons were performed using one-way analysis of variance (ANOVA) followed by Tukey's *post hoc* test via GraphPad Prism (Version 5). Statistical significance was set at $P<0.05$, $P<0.001$, and $P<0.0001$ (Adeneye *et al.*, 2021; 2024).

RESULTS

Effects of DH on the Average Body Weight and Percentage Weight Changes in DOX-Treated Rats

Repeated DOX injection on alternate days for 10 days resulted in significant ($P<0.05$) decreases in the average weight and percentage weight changes when compared to the untreated control normal rats (Table 2). However, oral pretreatment with 100 and 200 mg/kg/day DH significantly ($P<0.05$) reversed the weight loss dose relatedly while 50 mg/kg/day DH and 20 mg/kg/day SIL could not attenuate the DOX-induced weight losses (Table 2).

Effects of Graded Oral DH Doses on Liver Function Parameters (Serum Liver Enzymes, Total Protein, Albumin, and Total Bilirubin in DOX-Treated Rats

Intraperitoneal DOX injections at 3 mg/kg/day on alternate days for 10 consecutive days resulted in significant ($P<0.0001$) increases in the liver enzymes {alanine aminotransferase (AST), alanine aminotransferase (ALT) and alkaline phosphatase (ALP)}, and total bilirubin (TB) levels while causing significant ($P<0.05$) decreases in serum total protein (TP) and albumin (ALB) levels when compared to untreated normal control (Group I) values (Table 3). Oral DH pretreatment with 50, 100 and 200 mg/kg/day resulted in significantly ($P<0.05$, $P<0.001$ and $P<0.0001$) reversal in the DOX-induced liver function alterations and restoring them to about normal when compared with the values obtained for the untreated DOX-administered (Group II) rats (Table 3). SIL (used as the standard antioxidant drug) caused similar significant ($P<0.05$, $P<0.001$, and $P<0.0001$) improvement in the measured liver function parameters (Table 3).

Effects of Graded Oral DH Doses on the Renal Function Parameters (Serum Electrolytes: Na^+, K^+, and Cl^-; BUN and Cr) in DOX-treated Rats

Repeated intraperitoneal DOX injections on alternate days for 10 consecutive days resulted in significant ($P<0.001$) decreases in the serum Na^+ and Cl^- while it significantly ($P<0.001$, $P<0.0001$) increases serum K^+, BUN and Cr levels when compared to untreated normal control (Group I) values (Table 4). Oral pretreatments with 50, 100 and 200 mg/kg/day DH resulted in significantly ($P<0.05$, $P<0.001$ and $P<0.0001$) reversal in the DOX-induced renal function alterations and restoring them to about normal when compared with the values obtained for the untreated DOX-treated (Group II) rats (Table 4). SIL equally caused similar significant ($P<0.05$, $P<0.001$, and $P<0.0001$) improvement in the measured renal function parameters (Table 4).

Table 2: Effects of oral DH and SIL pretreatments on DOX-intoxicated rat weights and percentage body weight changes.

Groups	Treatments	Initial Weight (g)	Final Weight (g)	Weight Change (%)
I	10 mL/kg p.o. SW + 1 mL/kg i.p. SW	93.2±14.7	98.4±13.5	05.9±04.1
II	10 mL/kg p.o. SW + 3 mg/kg i.p. DOX	121.0±17.6	108.8±16.1^{a}	-09.9±06.8^{a}
III	200 mg/kg p.o. DH + 1 mL/kg i.p. DW	94.0±07.6	120.4±06.9^{c+}	28.4±07.2^{c+}
IV	50 mg/kg p.o. DH + 3 mg/kg i.p. DOX	101.2±16.6	81.4±19.4^{a-}	-11.3±11.8^{a-}
V	100 mg/kg p.o. DH + 3 mg/kg i.p. DOX	102.0±17.7	90.0±28.2^{a-}	-13.2±11.8^{a-}
VI	200 mg/kg p.o. DH + 3 mg/kg i.p. DOX	113.8±12.6	102.6±11.3^{a-}	-09.4±09.7^{a-}
VII	20 mg/kg p.o. SIL + 1 mL/kg i.p. DW	97.8±14.5	116.3±13.0	14.5±04.2^{b+}
VIII	20 mg/kg p.o. SIL + 3 mg/kg i.p. DOX	116.6±29.2	117.8±14.1	03.3±14.5

$^{a-}$ represents a significant decrease at P<0.05 when compared to untreated normal control (Group I) values; $^{b+}$ and $^{c+}$ represent significant increases when compared to the untreated doxorubicin (DOX) intoxicated rats. "Treatments" column represents doses in mL/kg for sterile water (SW) group or mg/kg for diosmin-hesperidin fixed-dose combination (DH), doxorubicin (DOX), and silymarin (SIL) groups. n = 6.

Table 3: Effects of graded oral DH doses and SIL on the liver function parameters (liver enzymes, total proteins, albumin and total bilirubin) in DOX-intoxicated rats.

Groups	Treatments	Na^+ (mmol/L)	K^+ (mmol/L)	Cl^- (mmol/L)	BUN (mg/dL)	Cr (µmol/L)
I	10 mL/kg p.o. SW + 1 mL/kg i.p. SW	136.4±2.0	05.0±0.1	97.2±1.4	07.5±0.5	16.0±1.2
II	10 mL/kg p.o. SW + 3 mg/kg i.p. DOX	126.7±0.3^{b}	08.1±0.7^{b+}	82.8±2.0^{a-}	17.9±0.8^{c+}	31.8±1.9^{c+}
III	200 mg/kg p.o. DH + 1 mL/kg i.p. DW	135.2±1.8$^{b\#}$	05.2±2.7^{b§}	96.8±0.6$^{a\#}$	04.9±0.3^{c§}	17.6±1.3^{c§}
IV	50 mg/kg p.o. DH + 3 mg/kg i.p. DOX	131.7±3.3$^{a\#}$	06.5±0.5^{a§}	87.7±2.2$^{a\#}$	14.8±2.1	17.1±2.1^{c§}
V	100 mg/kg p.o. DH + 3 mg/kg i.p. DOX	136.8±2.3$^{b\#}$	05.2±0.3^{b§}	95.7±1.0$^{a\#}$	10.5±2.4^{b§}	15.3±1.1^{c§}
VI	200 mg/kg p.o. DH + 3 mg/kg i.p. DOX	138.9±2.8$^{b\#}$	06.3±0.1^{a§}	103.7±1.9$^{b\#}$	08.9±1.2^{b§}	16.6±2.5^{c§}
VII	20 mg/kg p.o. SIL +1 mL/kg i.p. SW	138.8±1.4$^{b\#}$	04.8±0.2^{b§}	95.0±1.54$^{a\#}$	06.8±0.5^{c§}	20.6±2.8^{b§}
VIII	20 mg/kg p.o. SIL + 3 mg/kg i.p. DOX	131.6±6.1$^{a\#}$	06.1±0.4^{a§}	99.5±5.6$^{a\#}$	05.4±1.1^{c§}	20.5±2.8^{b§}

***P<0.0001 compared with same weight standard activated charcoal. "Treatments" column represents doses in mL/kg for sterile water (SW) group or mg/kg for diosmin-hesperidin fixed-dose combination (DH), doxorubicin (DOX), and silymarin (SIL) groups. n-value = 6.

Table 4: Effects of graded oral DH doses on the renal function parameters (electrolytes, BUN and Cr) in DOX-treated rats.

Groups	Treatment	Na^+ (mmol/L)	K^+ (mmol/L)	Cl^- (mmol/L)	BUN (mg/dL)	Cr (µmol/L)
I	10 mL/kg p.o. SW + 1 mL/kg i.p. SW	136.4±2.0	05.0±0.1	97.2±1.4	07.5±0.5	16.0±1.2
II	10 mL/kg p.o. SW + 3 mg/kg i.p. DOX	126.7±0.3^{b}	08.1±0.7^{b+}	82.8±2.0^{a-}	17.9±0.8^{c+}	31.8±1.9^{c+}
III	200 mg/kg p.o. DH + 1 mL/kg i.p. DW	135.2±1.8$^{b\#}$	05.2±2.7^{b§}	96.8±0.6$^{a\#}$	04.9±0.3^{c§}	17.6±1.3^{c§}
IV	50 mg/kg p.o. DH + 3 mg/kg i.p. DOX	131.7±3.3$^{a\#}$	06.5±0.5^{a§}	87.7±2.2$^{a\#}$	14.8±2.1	17.1±2.1^{c§}
V	100 mg/kg p.o. DH + 3 mg/kg i.p. DOX	136.8±2.3$^{b\#}$	05.2±0.3^{b§}	95.7±1.0$^{a\#}$	10.5±2.4^{b§}	15.3±1.1^{c§}
VI	200 mg/kg p.o. DH + 3 mg/kg i.p. DOX	138.9±2.8$^{b\#}$	06.3±0.1^{a§}	103.7±1.9$^{b\#}$	08.9±1.2^{b§}	16.6±2.5^{c§}
VII	20 mg/kg p.o. SIL +1 mL/kg i.p. SW	138.8±1.4$^{b\#}$	04.8±0.2^{b§}	95.0±1.54$^{a\#}$	06.8±0.5^{c§}	20.6±2.8^{b§}
VIII	20 mg/kg p.o. SIL + 3 mg/kg i.p. DOX	131.6±6.1$^{a\#}$	06.1±0.4^{a§}	99.5±5.6$^{a\#}$	05.4±1.1^{c§}	20.5±2.8^{b§}

$^{b+}$ and $^{c+}$ represent significant increases at P<0.001 and P<0.0001, respectively, while $^{a-}$ and $^{b-}$ represent significant decreases at P<0.05 and P<0.001, respectively, when compared to the untreated normal control (Group I) values. while $^{a\#}$ and $^{b\#}$ represent significant decreases at P<0.05 and P<0.001, respectively, when compared to untreated doxorubicin-intoxicated (Group II) rats. $^{a\S, b\S}$ and ^{c§} represent significant increases at P<0.05, P<0.001 and P<0.0001, respectively, when compared to the values for the untreated doxorubicin-intoxicated (Group II) rats. "Treatments" column represents doses in mL/kg for sterile water (SW) group or mg/kg for diosmin-hesperidin fixed-dose combination (DH), doxorubicin (DOX), and silymarin (SIL) groups. n = 6.

Effects of Graded Oral DH Doses and SIL on Hepatic and Renal Tissue SOD, CAT Activities, MDA and GSH Levels in DOX-treated Rats

Table 5 represents the effect of the oral DH and SIL pretreatments on the hepatic antioxidant activities in DOX-treated rats. DOX intoxication caused significant (P<0.0001) increases in the CAT activity and MDA levels while it significantly (P<0.05) decreased the hepatic tissue SOD activity and GSH levels when compared to the untreated normal control (Group I) rats (Table 5). However, DH pretreatment significantly (P<0.05, P<0.001, P<0.0001) reversed the altered level in a dose related fashion (Table 5). Similarly, DOX intoxication caused significant (P<0.0001) increases in the CAT activity and MDA levels while it significantly (P<0.05) decreased the hepatic tissue SOD activity and GSH levels when compared to the untreated normal control (Group I) rats (Table 6). Also, DH pretreatment significantly (P<0.05, P<0.001, P<0.0001) reversed the altered levels in a dose related fashion (Table 6).

Effects of Graded Oral DH Doses on the Hepatic and Renal Tissue Pro-Inflammatory Markers in DOX-Treated Rats

DOX intoxication caused a significant (P<0.0001) increase in the hepatic tissue TNF-α level compared to the normal control group, indicating heightened DOX-induced inflammation (Table 7). However, oral pretreatment with graded oral DH doses caused significant (P<0.05, P<0.001, P<0.0001) dose-dependent reduction in the hepatic tissue TNF-α level compared to the DOX-intoxicated group and demonstrating the ability of DH to suppress inflammation, with the highest dose (200 mg/kg) showing the most profound suppression (Table 7). Equally, SIL pretreatment reduced TNF-α levels, though less effectively than the highest dose of DH (Table 7). Similarly, DOX intoxication caused a significant (P<0.0001) reduction in the hepatic tissue IL-10 levels compared to the untreated normal control, reflecting impaired anti-inflammatory defense mechanisms (Table 7). Oral pretreatment with graded oral DH doses caused a dose-dependent elevation in the hepatic tissue IL-10 levels, indicating enhanced activation of anti-inflammatory pathways by DH pre-treatment, with the 200 mg/kg dose restoring IL-10 to near-normal levels (Table 7). However, oral SIL pretreatment caused a moderate (P<0.001) increase in IL-10 levels compared to the DOX-only treated group, suggesting some protective effects, though not as pronounced as DH at higher doses (Table 7). Similar patterns were recorded for the renal tissue TNF-alpha in the untreated DOX-only and DH-pretreated-DOX-treated rats.

Table 5: Effects of DH pretreatment and SIL on the hepatic tissue antioxidant profile in DOX-treated rats.

Groups	Treatment	CAT (U/mg Protein)	SOD (U/ mg Protein)	MDA (nmol/mg Protein)	GSH (µmol/mL)
I	10 mL/kg p.o. SW + 1 mL/kg i.p. SW	04.2 ± 0.5	147.0 ± 16.2	05.0 ± 0.2	08.8 ± 0.8
II	10 mL/kg p.o. SW + 3 mg/kg i.p. DOX	14.0 ± 1.6^{c+}	51.1 ± 3.3^{c-}	13.6 ± 0.5^{c+}	02.7 ± 0.5^{c-}
III	200 mg/kg p.o. DH + 1 mL/kg i.p. DW	03.3 ± 0.3$^{c§-}$	95.5 ± 4.7^{b+}	05.9 ± 0.5$^{c§-}$	10.3 ± 0.2^{c+}
IV	50 mg/kg p.o. DH + 3 mg/kg i.p. DOX	08.8 ± 0.8$^{b§-}$	58.8 ± 8.7^{c-}	09.3 ± 0.4$^{a§-}$	05.5 ± 0.6^{a+}
V	100 mg/kg p.o. DH + 3 mg/kg i.p. DOX	05.5 ± 1.5$^{c§-}$	61.6 ± 3.4^{a-}	07.2 ± 0.7$^{b§-}$	07.4 ± 1.2^{b+}
VI	200 mg/kg p.o. DH + 3 mg/kg i.p. DOX	05.0 ± 0.7$^{c§-}$	68.5 ± 1.9^{a-}	06.2 ± 0.8$^{b§-}$	09.5 ± 0.2^{c+}
VII	20 mg/kg p.o. SIL +1 mL/kg i.p. SW	04.5 ± 0.7$^{c§-}$	38.7 ± 2.7^{c-}	08.6 ± 0.5^{c§}	06.5 ± 0.7^{b+}
VIII	20 mg/kg p.o. SIL + 3 mg/kg i.p. DOX	05.5 ± 1.1$^{c§-}$	79.5 ± 1.2$^{a\#}$	05.8 ± 0.9$^{c§-}$	07.5 ± 0.2^{b+}

$^{c+}$ represents a significant increase at P<0.0001 while $^{c-}$ represents a significant decrease at P<0.001 when compared to untreated normal control (Group I) rats. $^{a§-, b§-}$ and $^{c§-}$ represent significant decreases at P<0.05, P<0.001 and P<0.0001, respectively, while $^{a+, b+,}$ and $^{c+}$ represent significant increases at P<0.05, P<0.001, and P<0.0001 when compared to doxorubicin-only treated control (Group II) values, respectively. "Treatments" column represents doses in mL/kg for sterile water (SW) group or mg/kg for diosmin-hesperidin fixed-dose combination (DH), doxorubicin (DOX), and silymarin (SIL) groups. n = 6.

Histopathological Studies of the Effects of Graded Oral DH Doses and SIL on the Hepatic Tissues of DOX-Treated Rats

The photomicrograph of the normal hepatic tissues showed normal hepatocytes radially arranged from the hepatic margins toward the center vein along with the portal triads with each column interspaced by liver sinusoids (Figure 1A). Repeated intraperitoneal DOX injections with 3 mg/kg of DOX on alternate days for 10 days was associated with distortion of the liver cytoarchitecture, characterized with cellular degeneration and pyknotic cells. The hepatic tissues of the groups treated with DOX-only caused degenerative changes in the liver parenchyma with each column interspaced by liver sinusoids with the dilatations of portal vein and hepatic artery (Figure 1B). While repeated oral DH pretreatment caused no distortion in hepatic cytoarchitecture (Figure 1C), the hepatic tissues of the

groups treated with 50 mg/kg/day DH showed a slight recovery of hepatocytes with the portal triads dilatation (Figure 1D). Similarly, in the hepatic tissues pretreated with 100 mg/kg/day DH before the DOX intoxication, there was a moderate distortion in liver cytoarchitecture with the hepatocytes sparsely arranged from the hepatic lobules and portal triads dilatation (Figure 1E). However, in the group pretreated with 200 mg/kg/day DH before DOX intoxication, there was a mild distortion of the liver cytoarchitecture, characterized by the absence of remarkable cellular degeneration and pyknotic cells (Figure 1F). The hepatic tissues of the groups treated with 20 mg/kg/day SIL-only showed a normal liver parenchyma with well-structured hepatocytes and portal triads toward the center vein along with each column interspaced by liver sinusoids (Figure 1G). The hepatic tissues of the groups pretreated with 20 mg/kg/day SIL and DOX intoxication showed complete restoration of liver parenchyma following the reversal of the degenerative changes of the liver parenchyma with each column interspaced by liver sinusoids (Figure 1H).

Table 6: Effects of DH pretreatment and SIL on the renal tissue antioxidant profile in DOX-treated rats.

Groups	Treatment	CAT (U/mg Protein)	SOD (U/ mg protein)	MDA (nmol/mg Protein)	GSH (µmol/mL)
I	10 mL/kg p.o. SW + 1 mL/kg i.p. SW	02.6 ± 0.3	27.6 ± 4.7	01.4 ± 0.3	15.0 ± 0.4
II	10 mL/kg p.o. SW + 3 mg/kg i.p. DOX	4.6 ± 0.6^{c+}	15.5 ± 1.4^{c-}	08.9 ± 1.6^{c+}	06.0 ± 1.0^{c-}
III	200 mg/kg p.o. DH + 1 mL/kg i.p. DW	01.6 ± 0.2$^{b\S-}$	34.9 ± 3.1$^{b\#}$	01.0 ± 0.2$^{c\S-}$	13.4 ± 0.2$^{b\#}$
IV	50 mg/kg p.o. DH + 3 mg/kg i.p. DOX	03.4 ± 0.5	23.8 ± 1.6$^{a\#}$	02.8 ± 0.4$^{c\S-}$	09.5 ± 1.1$^{a\#}$
V	100 mg/kg p.o. DH + 3 mg/kg i.p. DOX	02.5 ± 0.3$^{a\S-}$	31.4 ± 4.1$^{b\#}$	01.6 ± 0.1$^{c\S-}$	15.9 ± 0.2$^{c\#}$
VI	200 mg/kg p.o. DH + 3 mg/kg i.p. DOX	01.8 ± 0.2$^{b\S-}$	56.2 ± 5.8$^{b\#}$	01.0 ± 0.1$^{c\S-}$	20.5 ± 1.0$^{c\#}$
VII	20 mg/kg p.o. SIL +1 mL/kg i.p. SW	01.5 ± 0.2$^{b\S-}$	36.9 ± 3.9$^{b\#}$	02.1 ± 0.6$^{c\S-}$	15.2 ± 1.9$^{c\#}$
VIII	20 mg/kg p.o. SIL + 3 mg/kg i.p. DOX	02.8 ± 0.4$^{a\S-}$	27.9 ± 5.6$^{a\#}$	01.0 ± 0.1$^{c\S-}$	14.5 ± 0.5$^{b\#}$

$^{c+}$ represents a significant increase at $P<0.0001$ while $^{c-}$ represents a significant decrease at $P<0.001$ when compared to untreated normal control (Group I) rats. $^{a\S-, b\S-}$ and $^{c\S-}$ represent significant decreases at $P<0.05$, $P<0.001$ and $P<0.0001$, respectively, while $^{a\#, b\#,}$ and $^{c\#}$ represent significant increases at $P<0.05$, $P<0.001$, and $P<0.0001$ when compared to the untreated doxorubicin-intoxicated control (Group II) values, respectively. "Treatments" column represents doses in mL/kg for sterile water (SW) group or mg/kg for diosmin-hesperidin fixed-dose combination (DH), doxorubicin (DOX), and silymarin (SIL) groups. n = 6.

Table 7: Effects of DH and SIL pretreatment on the hepatic tissue inflammatory markers (TNF-α and IL-10) in DOX intoxicated rats.

Groups	Treatment given	TNF-α (pg/mL)	IL-10 (pg/ mL)
I	10 mL/kg p.o. SW + 1 mL/kg i.p. SW	12.0 ± 1.2	16.7 ± 0.8
II	10 mL/kg p.o. SW + 3 mg/kg i.p. DOX	50.0 ± 4.0^{c+}	07.0 ± 0.7^{a-}
III	200 mg/kg p.o. DH + 1 mL/kg i.p. DW	10.8 ± 1.0$^{c\S-}$	22.7 ± 1.8$^{b\#}$
IV	50 mg/kg p.o. DH + 3mg/kg i.p. DOX	41.0 ± 2.4 $^{a\S-}$	09.5 ± 0.7$^{a-,a\#}$
V	100 mg/kg p.o. DH + 3 mg/kg i.p. DOX	24.3 ± 1.0$^{b\S-}$	27.2 ± 1.3$^{b\#}$
VI	200 mg/kg p.o. DH + 3 mg/kg i.p. DOX	15.8 ± 2.0$^{c\S-}$	30.8 ± 1.3$^{c\#}$
VII	20 mg/kg p.o. SIL + 1 mL/kg i.p. SW	15.7 ± 1.0$^{c\S-}$	37.7 ± 1.3$^{a\#}$
VIII	20 mg/kg p.o. SIL + 3 mg/kg i.p. DOX	35.8 ± 1.9$^{a\S-}$	22.7 ± 2.2$^{b\#}$

$^{c+}$ represents a significant increase at $P<0.0001$ while $^{a-}$ represents a significant decrease at $P<0.05$ when compared to untreated normal control (Group I) rats. $^{a\S-, b\S-}$ and $^{c\S-}$ represent significant decreases at $P<0.05$, $P<0.001$ and $P<0.0001$, respectively, while $^{a\#, b\#,}$ and $^{c\#}$ represent significant increases at $P<0.05$, $P<0.001$, and $P<0.0001$ when compared to the untreated DOX-intoxicated control (Group II) values, respectively. "Treatments" column represents doses in mL/kg for sterile water (SW) group or mg/kg for diosmin-hesperidin fixed-dose combination (DH), doxorubicin (DOX), and silymarin (SIL) groups. n = 6.

Table 8: Effects of DH and SIL pretreatment on the renal tissue inflammatory markers (TNF-α and IL-10) in DOX-treated rats.

Groups	Treatment given	TNF-α (pg/mL)	IL-10 (pg/ mL)
I	10 mL/kg p.o. SW + 1 mL/kg i.p. SW	09.7 ± 1.0	14.3 ± 1.1
II	10 mL/kg p.o. SW + 3 mg/kg i.p. DOX	59.8 ± 2.6^{c+}	09.5 ± 1.3^{a-}
III	200 mg/kg p.o. DH + 1 mL/kg i.p. DW	12.3 ± 0.9$^{c\S-}$	20.5 ± 0.9$^{a\#}$
IV	50 mg/kg p.o. DH + 3mg/kg i.p. DOX	45.8 ± 1.7 $^{a\S-}$	15.7 ± 2.5$^{a\#}$
V	100 mg/kg p.o. DH + 3 mg/kg i.p. DOX	23.5 ± 4.5$^{b\S-}$	28.0 ± 1.4$^{b\#}$
VI	200 mg/kg p.o. DH + 3 mg/kg i.p. DOX	21.7 ± 1.1$^{c\S-}$	36.0 ± 1.1$^{c\#}$
VII	20 mg/kg p.o. SIL + 1 mL/kg i.p. SW	13.5 ± 1.2$^{c\S-}$	39.8 ± 1.0$^{c\#}$
VIII	20 mg/kg p.o. SIL + 3 mg/kg i.p. DOX	28.8 ± 2.2$^{b\S-}$	31.5 ± 3.1$^{a\#}$

$^{c+}$ represents a significant increase at $P<0.0001$ while $^{a-}$ represents a significant decrease at $P<0.05$ when compared to untreated normal control (Group I) rats. $^{a\S-,\ b\S-}$ and $^{c\S-}$ represent significant decreases at $P<0.05$, $P<0.001$ and $P<0.0001$, respectively, while $^{a\#,\ b\#,}$ and $^{c\#}$ represent significant increases at $P<0.05$, $P<0.001$, and $P<0.0001$ when compared to the untreated DOX-intoxicated control (Group II) values, respectively. "Treatments" column represents doses in mL/kg for sterile water (SW) group or mg/kg for diosmin-hesperidin fixed-dose combination (DH), doxorubicin (DOX), and silymarin (SIL) groups. n = 6.

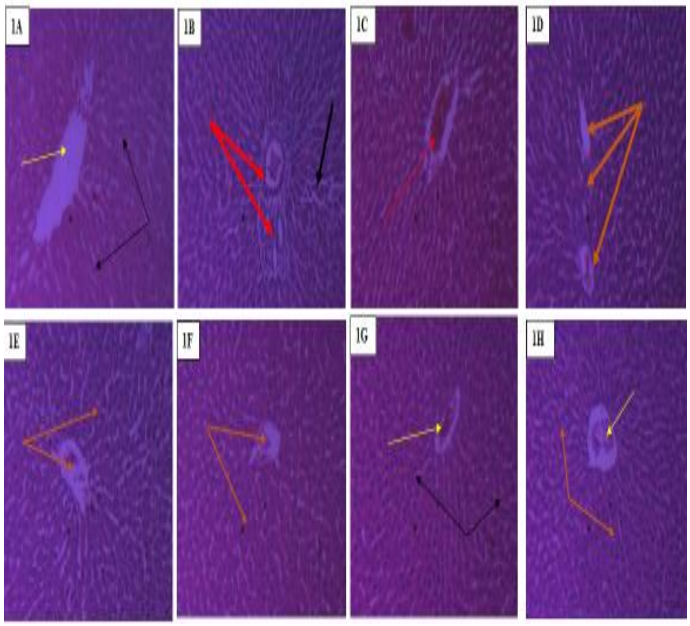

Figure 1A-1H: Histopathological effects of DH and SIL pretreatment on the DOX-intoxicated rat hepatic tissue. Cross-sectional photomicrographs of an untreated normal rat hepatic tissue showing normal hepatocytes (thin black arrow) and central hepatic vein (thin yellow arrow) **(Figure 1A)**; treated with 3 mg/k/day/i.p. DOX-only showing severe periportal congestion and lymphocytic infiltration (thin red arrow) and severe sinusoidal congestion (thick black arrow) **(Figure 1B)**; rat liver treated with 200 mg/kg/day DH showing mild central hepatic vein congestion **(Figure 1C)**, pretreated with 50 mg/kg/day DH before treatment with 3 mg/kg/day DOX showing moderate-to-severe sinusoidal congestion (thick brown arrow) **(Figure 1D)**; hepatic tissue pretreated with 100 mg/kg/day DH before DOX-intoxication showing mild-to-moderate sinusoidal congestion (thin brown arrow) **(Figure 1E)**; pretreated with 200 mg/kg/day DH before DOX-intoxication showing mild sinusoidal congestion (thin brown arrow) and normal hepatocytes **(Figure 1F)**; pretreated with 20 mg/kg/day SIL-only showing normal hepatic central vein (thin yellow arrow) and hepatocytes (thin black arrow) **(Figure 1G)**, pretreated with 20 mg/kg/day SIL before DOX-intoxication showing **(Figure 1H)** (×100 magnification, stained with H & E stains).

Effects of Graded Oral DH Doses on the Hepatic and Effects of Graded Oral DH Doses and SIL on the Histopathology of the Renal Tissues of DOX-Treated Rats

The photomicrograph of the normal renal tissues showed normal tubulo-glomerular and interstitial cytoarchitecture (Figure 2A). Repeated DOX treatment of rats caused severe tubulo-glomerular degeneration. Diffuse tubular necrosis, cystic tubular dilatation and fatty infiltration were observed significantly in the Bowman's capsule (Figure 2B). The renal tissue of the group pretreated with 200 mg/kg/day DH showed normal renal tubular and glomerular cells that were properly embedded in the Bowman's capsule (Figure 2C). The renal tissue of the groups repeatedly treated with 3 mg/kg DOX and 50 mg/kg/day DH showed moderate-to severe focal tubular necrosis, tubular cystic dilatation and fatty infiltration of the Bowman's capsule (Figure 2D).

Similarly, the kidney tissues of rats pretreated with 100 mg/kg/day DH before treatment with 3 mg/kg/day DOX showed poor renal tubules, distorted glomeruli and Bowman's capsule (Figure 2E). In rats that were pretreated with 200 mg/kg/day DH before DOX intoxication, there was a complete restoration of renal tubules that was evidenced by the reversal of the degenerative changes of the glomerular parenchyma (Figure 2F). With 20 mg/kg/day SIL-only pretreatment, the renal tissues revealed renal tubular and glomerular distortion as the cells were not properly embedded in the Bowman's capsule (Figure 2G). The renal tissues of the group pretreated with 20 mg/kg/day of SIL revealed improved renal cytoarchitecture that was characterized by mild tubulo-glomerular degeneration, focal tubular necrosis, and mild fatty infiltration of the Bowman's capsule (Figure 2H).

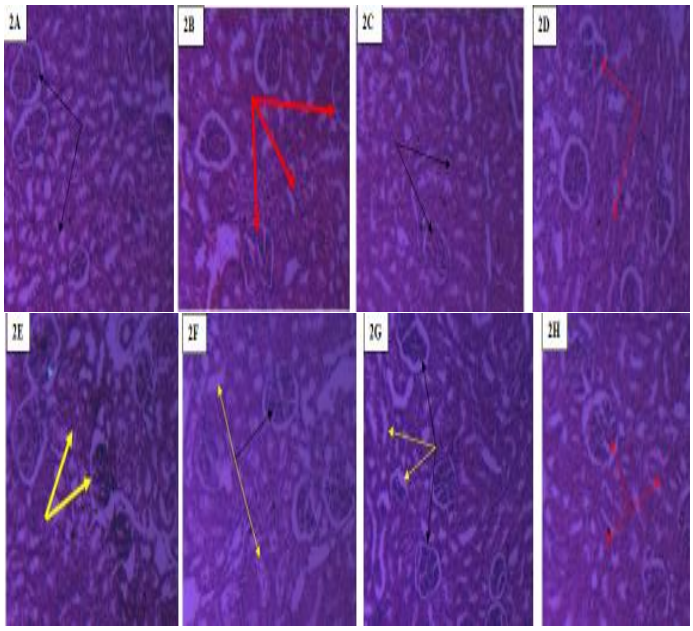

Figure 2A-2H: Histopathological effects of DH and SIL pretreatment on the DOX-intoxicated rat renal tissue. Cross-sectional photomicrographs of the renal tissue of untreated normal control rat showing normal glomerular and tubular histoarchitecture (thin black arrow) **(Figure 2A)**; DOX-only intoxicated rat renal tissue showing severe diffuse tubulo-glomerular congestion and degeneration (thick red arrow) **(Figure 2B)**; 200 mg/kg/day DH-pretreated renal tissue showing normal renal histoarchitecture (thin black arrows) **(Figure 2C)**; 50 mg/kg/day DH pretreated renal tissue before DOX-intoxication showing moderate-to-severe tubulo-glomerular degeneration (thin red arrow) **(Figure 2D)**; 100 mg/kg/day DH pretreated renal tissue before DOX-intoxication showing mild-to-moderate focal tubulo-glomerular necrosis (thick yellow arrow) **(Figure 2E)**; 200 mg/kg/day DH pretreated renal tissue before DOX-intoxication showing a complete restoration of renal tubules showing mild tubular degeneration ((thin yellow arrow) and normal glomerular parenchyma that are properly embedded in the Bowman's capsule (thin black arrow) **(Figure 2F)**; 20 mg/kg/day SIL-only pretreated renal tissue showing mild renal tubular congestion and normal glomeruli **(Figure 2G)**; 20 mg/kg/day of SIL-pretreated DOX-intoxicated renal tissue showing improved renal histoarchitecture that was characterized by mild tubulo-glomerular degeneration (thin red arrow) **(Figure. 2H)** (×100 magnification, stained with hematoxylin & eosin stains).

DISCUSSION

DOX, an anthracycline antibiotic, has historically been a cornerstone in the management of advanced malignancies, including sarcomas, breast, and ovarian cancers (Radford, 2024). Its combination regimens with other chemotherapeutic agents have demonstrably improved long-term patient survival outcomes.

Despite its significant antineoplastic efficacy, the clinical utility of DOX is severely constrained by its off-target systemic toxicity to non-cancerous tissues. Following intravenous administration, DOX is characterized by rapid systemic clearance and preferential accumulation within the hepatic and renal systems (Pugazhendhi *et al.*, 2018). These organs are not merely sites of accumulation; they also fulfill the primary roles in the metabolism and excretion of DOX (Oliveira *et al.*, 2020; Pippa *et al.*, 2020). This drug disposition and biotransformation within the liver and kidneys initiate a cascade of organ injury marked by inflammation and oxidative stress, promoting cytotoxic cellular signaling (Boeno *et al.*, 2023).

The precise mechanisms underlying DOX-induced nephrotoxicity and hepatotoxicity remain under investigation, but current hypotheses center on the local accumulation and subsequent metabolism of DOX, which culminates in free radical generation and resulting lipid peroxidation; accelerated cellular apoptosis (Yang *et al.*, 2019; Renu *et al.*, 2021; vander Zanden *et al.*, 2021; Kong *et al.*, 2022); and mitochondrial dysfunction (Kong *et al.*, 2022).

The resulting multi-organ toxicity necessitates the development of therapeutic strategies capable of preserving DOX antitumor efficacy while mitigating its deleterious systemic effects. Currently, there are no clinical therapies approved for the prevention or treatment of DOX-induced hepatorenal toxicity (Boeno *et al.*, 2023).

In the present study, DOX hepatorenal toxicity was reliably established via repeated intraperitoneal injections of DOX (3 mg/kg/day, administered on alternate days for 10 days). This regimen consistently resulted in biochemical hallmarks of organ dysfunction, including elevated serum urea and creatinine levels, and electrolyte imbalance (Adeneye *et al.*, 2021; Ikewuchi *et al.*, 2022; Jomova *et al.*, 2023; Olorundare *et al.*, 2024). Furthermore, DOX toxicity was characterized by significant derangement of oxidative stress markers in both hepatic and renal tissues (Adeneye *et al.*, 2021; Ikewuchi *et al.*, 2022; Olorundare *et al.*, 2024). However, the observed biochemical alterations were robustly supported by histopathological lesions, including hepatocyte degeneration (in the liver), severe tubulo-glomerular degeneration, focal tubular necrosis, tubular cystic dilatation, and glomerular congestion (in the kidneys).

The underlying molecular culprits for DOX-mediated hepatorenal injury are primarily mediated via multiple mechanisms including reactive oxygen species (ROS) release since the metabolism and excretion of DOX lead to the production of ROS, which overwhelm the native antioxidant defense systems, inducing redox imbalance and oxidative stress (Mansouri *et al.*, 2017; Jomova *et al.*, 2023); accelerated apoptosis since DOX promotes apoptosis through the upregulation of pro-apoptotic protein expression (Xiang *et al.*, 2021); as well as inflammation since DOX triggers an inflammatory response, evidenced by elevated expression of several pro-inflammatory cytokines in the affected liver and renal tissues (Song *et al.*, 2019). Therefore, therapeutic strategies targeting the inhibition of oxidative stress, apoptosis, and inflammation

represent a promising avenue for preventing DOX-induced hepatorenal toxicity.

A key finding of this investigation was the profound impact of DOX intoxication on tissue antioxidant status: notable increases in the activity of superoxide dismutase (SOD), catalase (CAT), and glutathione peroxidase (GPx), alongside a significant decrease in reduced glutathione (GSH) levels (in agreement with Arunachalam *et al.*, 2022). Additionally, DOX significantly elevated malondialdehyde (MDA), a key marker of lipid peroxidation.

The fact that repeated oral pretreatment with the fixed-dose combination of diosmin and hesperidin (DH) significantly ameliorated these measured biochemical and histological derangements strongly indicates the inherent chemoprotective potential of DH against DOX-induced hepatorenal injury. This effect was most likely mediated through the antioxidant/free radical scavenging activity of the constituent flavonoids.

Specifically, DH pretreatment remarkably protected the oxidative stress markers (SOD, CAT, and MDA) from DOX-mediated increases in their tissue activities, suggesting a potent antioxidative action comparable to that of the reference standard antioxidant, Silymarin (SIL).

Diosmin (diosmetin 7-O-rutinoside) is a flavone glycoside found abundantly in citrus plants, recognized for its potent antioxidant properties (Guo *et al.*, 2024). Its molecular formula is $C_{28}H_{32}O_{15}$ with a molecular weight of 608.549 g/mol and IUPAC name: 5 hydroxy-2-(3-hydroxy-4-methoxyphenyl)-7-[(2S,3R,4S,5S,6R)-3,4,5-trihydroxy-6-[[(2R,3R,4R,5R,6S)-3,4,5-trihydroxy-6-methyloxan-2-yl]oxymethyl]oxan-2-yl]oxychromen-4-one (Mustafa *et al.*, 2022). Beyond its antioxidant capacity, *in vitro* and *in vivo* studies have validated a broad spectrum of biological activities for diosmin, including antihyperglycemic, anti-inflammatory, analgesic, anticancer, anti-ulcer, immunomodulatory, anti-parasitic, and antimicrobial properties (Huwait and Mobashir, 2022; Mustafa *et al.*, 2022; Guo *et al.*, 2024). Previous research has already established the protective effect of diosmin against DOX-induced hepatorenal toxicity by enhancing antioxidant mechanisms, reducing inflammation and apoptosis, and restoring organ architecture (Ali *et al.*, 2021; Mansour *et al.*, 2024). Similarly, hesperidin has been reported to confer protection against DOX nephrotoxicity in rodent models by effectively limiting lipid peroxidation in both hepatic and renal tissues (Tammam *et al.*, 2022; Alherz *et al.*, 2024).

The effective amelioration of DOX-mediated hepatorenal dysfunctions by DH in the dose range of 50-200 mg/kg/day highlights its promising therapeutic potential in mitigating DOX-induced toxicity, primarily through antioxidant/free radical scavenging and anti-inflammatory mechanisms.

CONCLUSION

In summary, this study reaffirms that DOX, despite its potent antineoplastic activity, induces significant systemic toxicity, specifically pronounced hepatorenal injury, primarily mediated by oxidative stress, inflammation, and accelerated apoptosis. The findings demonstrate that pretreatment with the fixed-dose combination of diosmin and hesperidin (DH) effectively and reliably ameliorates the DOX-induced biochemical and histopathological derangements in both the liver and kidneys. This protective effect is comparable to the standard antioxidant silymarin. The chemoprotective potential of DH is strongly linked to its inherent antioxidant and free radical scavenging properties, alongside its capacity to mitigate the pro-inflammatory and pro-apoptotic signaling triggered by DOX metabolism. Given the current lack of approved clinical therapies for DOX hepatorenal toxicity, the robust evidence presented here highlights DH (at 50-200 mg/kg/day) as a promising and pharmacologically relevant therapeutic candidate for clinical translation to preserve organ integrity and enhance the overall safety profile of DOX-based chemotherapy regimens.

ABBREVIATIONS

%Δwt: Percentage weight change, **ALB**: Albumin, **ALP**: Alkaline phosphatase, **ALT**: Alanine aminotransferase, **AST**: Aspartate aminotransferase, **BUN**: Blood urea nitrogen, **CAT**: Catalase, **Cr**: Creatinine, **DH**: 90% diosmin-10% hesperidin fixed-dose combination, **DOX**: Doxorubicin, **GSH**: Reduced glutathione, **IL-10**: Interleukin-10, ***i.p.***: Intraperitoneal route, **LASUCOM**: Lagos State University College of Medicine, **LASUREC**: Lagos State University Research Ethics Committee, **MDA**: Malondialdehyde, ***p.o.***: *Per os,* **S.D**.: Standard deviation, **S.E.M**.: Standard error of the mean, **SIL**: Silymarin**, SOD**: Superoxide dismutase, **TB**: Total bilirubin, TP: Total protein, **TNF-α**: Tumor necrosis factor-alpha.

ACKNOWLEDGMENTS

The authors appreciate the immense contribution of Mr. Samuel Kayode Akindele, Deputy Director, Medical Laboratory Services, Nigerian Institute of Medical Research, Yaba, Lagos State, Nigeria, for his technical assistance in the assays of the antioxidant and inflammatory markers; Mrs. Juliana Ogundipe and other staff of the Animal House, Lagos State University College of Medicine, Ikeja, Lagos State, Nigeria, for the care, handling of experimental rats and disposing the rat carcasses after the experiment was terminated.

AUTHORS' CONTRIBUTION

Conception and design: AAA, SF, and NGA.; Acquisition of data: AAA, SF, and NGA; Analysis, interpretation of data and drafting of the manuscript: AAA, FS, NGA, AO, and IIO; Revising for intellectual content: AAA, FS and NGA; Final approval: AAA, FS, NGA, AO, and IIO. All authors read and agreed to publish the manuscript.

CONFLICT OF INTEREST

The authors declare no competing interests.

FUNDING

No funding was received for this research.

AUTHORS' DECLARATION

The authors declare that this work is original and that any liability for claims relating to the content of this article will be borne by them.

REFERENCES

Abd-Ellatif RN, Nasef NA, El-Horany HE, Emam MN, Younis RL, El Gheit REA, Elseady W, Radwan DA, Hafez YM, Eissa A, Aboalsoud A, Shalaby RH, Atef MM (2022). Adrenomedullin mitigates doxorubicin-induced nephrotoxicity in rats: Role of oxidative stress, inflammation, apoptosis, and pyroptosis. *International Journal of Molecular Science* 23(23): 14570. http://doi.org/10.3390/ijms232314570.

Adeneye AA, Babatope FE, Adesiji-Adelekan AE, Olorundare OE, Okoye II (2024). Tadalafil pretreatment attenuates doxorubicin-induced hepatorenal toxicity by modulating oxidative stress and inflammation in Wistar rats. *Toxicology Report* 13: 101737. https://doi.org/10.1016/j.toxrep.2024.101737

Adeneye AA, Olorundare OE, Akinsola AO, Sanni DA, Okoye II, Ntambi JM, Mukhtar H (2021). Ameliorative potential of *Clerodendrum volubile* ethanol leaf extract on doxorubicin-induced hepatorenal toxicities in rats. *Pharmacology and Toxicology of Natural Medicine* 1(1): 1-13. https://doi.org/10.52406/ptnm.v1i1.8

Afsar T, Razak S, Almajwal A, Al-Disi D (2020). Doxorubicin-induced alterations in kidney functioning, oxidative stress, DNA damage, and renal tissue morphology: Improvement by *Acacia hydaspica* tannin-rich ethyl acetate fraction. *Saudi Journal of Biological Sciences* 27(9): 2251-2260. https://doi.org/10.1016/j.sjbs.2020.07.011

Aggarwal V, Tuli HS, Thakral F, Singhal P, Aggarwal D, Srivastava S, Pandey A, Sak K, Varol M, Khan MA, Sethi G (2020). Molecular mechanisms of action of hesperidin in cancer: Recent trends and advancements. *Experimental Biology and Medicine (Maywood)* 245(5): 486-497. https://doi.org/10.1177/1535370220903671

Alherz FA, El-Masry TA, Oriquat GA, Elekhnawy E, Al-Shaalan NH, Gaballa MMS, El Zahaby EI, El-Nagar MMF (2024). Hesperidin nanoformulation: A potential strategy for reducing doxorubicin-induced renal damage via the Sirt-1/HIF1-α/VEGF/NF-κB signalingcascade. *Pharmaceuticals* 17(9): 1144. https://doi.org/10.3390/ph17091144

Alherz FA, Negm WA, El-Masry TA, Elmorshedy KE, Al-Kadem AH (2023). The potential beneficial role of Ginkgetin in doxorubicin-induced hepatotoxicity: Elucidating the underlying claim. *Biomed Pharmacotherapy* 165: 115010. https://doi.org/10.1016/j.biopha.2023.115010

Ali N, AlAsmari, AF, Imam F, Ahmed MZ, Alqahtani F, Alharbi M, AlSwayyed M, AlAsmari F, Alasmari M, Alshammari A, Fantoukh OI, Alanazi MM (2021). Protective effect of diosmin against doxorubicin-induced nephrotoxicity. *Saudi Journal of Biological Sciences* 28(8): 4375-83. https://doi.org/10.1016/j.sjbs.2021.04.030

Arunachalam S, Nagoor Meeran MF, Azimullah S, Jha NK, Saraswathiamma D, Subramanya S, Albawardi A, Ojha S (2022). α-Bisabolol attenuates doxorubicin induced renal toxicity by modulating NF-κB/MAPK signaling and caspase-dependent apoptosis in rats. *International Journal of Molecular Sciences* 23(18): 10528. https://doi.org/10.3390/ijms231810528

Boeno FP, Patel J, Montalvo RN, Lapierre-Nguyen SS, Schreiber CM, Smuder AJ (2023). Effects of exercise preconditioning on doxorubicin-induced liver and kidney toxicity in male and female rats. *International Journal of Molecular Science* 24(12): 10222. https://doi.org/10.3390/ijms241210222

Bogucka-Kocka, A, Woźniak M, Feldo M, Kockic J, Szewczyk K (2013). Diosmin - isolation techniques, determination in plant material and pharmaceutical formulations, and clinical use. *Natural Product Communications* 8(4): 545-50. https://doi.org/10.1177/1934578X1300800435

Carballo-Villalobos AI, González-Trujano M-E, Pellicer F, López-Muñoz FJ (2016). Antihyperalgesic effect of hesperidin improves with diosmin in experimental

neuropathic pain. *BioMed Research International* 2016: 8263463. https://doi.org/10.1155/2016/8263463

D'Angelo NA, Noronha MA, Câmara MCC, Kurnik IS, Feng C, Araujon VHS, Santos JHPM, Feitosa V, Molino JVD, Rangel-Yagui CO, Chorilli M, Ho EA, Lopes AM (2022). Doxorubicin nanoformulations on therapy against cancer: An overview from the last 10 years. *Biomaterials Advances* 133: 112623. https://doi.org/10.1016/j.msec.2021.112623

Faezi M, Motavalizadehkakhky A, Tabrizi MH, Dolatabadi S, Es-haghi A (2025). Zein-sodium caseinate-diosmin nanoparticles as a promising anticancer agent with targeted efficacy against A2780 cell line. *Scientific Reports* 15: 8762. https://doi.org/10.1038/s41598-025-93772-1

Gerges SH, Wahdan SA, Elsherbiny DA, El-Demerdash E (2022). Pharmacology of diosmin, a citrus flavone glycoside: An updated review. *European Journal of Drug Metabolism & Pharmacokinetics* 47(1): 1-18. https://doi.org/10.1007/s13318-021-00731-y

Gölboyu BE, Erdoğan MA, Çoşar MA, Balıkoğlu E, Erbaş O (2024). Diosmin and hesperidin have a protective effect in diabetic neuropathy via the FGF21 and galectin-3 pathway. *Medicina (Kaunas)* 60(10): 1580. https://doi.org/10.3390/medicina60101580

Guo C, Wan L, Li C, Wen Y, Pan H, Zhao M, Wang J, Ma X, Nian Q, Tang J, Zeng J (2024). Natural products for gastric carcinoma prevention and treatment: Focus on their antioxidant stress actions in the Correa's cascade. *Phytomedicine* 123: 155253. https://doi.org/10.1016/j.phymed.2023.155253

Guo H, Liu Y, Wang L, Zhang G, Su S, Zhang R, Zhang J, Li A, Shang C, Bi B, Li, Z (2016). Alleviation of doxorubicin-induced hepatorenal toxicities with sesamin via the suppression of oxidative stress. *Human & Experimental Toxicology* 35(11): 1183-93. https://doi.org/10.1177/0960327115626581

Huwait E, Mobashir M (2022). Potential and therapeutic roles of diosmin in human diseases. *Biomedicines* 10(5): 1076. https://doi.org/10.3390/biomedicines10051076

Ikewuchi CC, Ifeanacho MO, Ikewuchi JC (2021). Moderation of doxorubicin-induced nephrotoxicity in Wistar rats by aqueous leaf-extracts of *Chromolaena odorata* and *Tridax procumbens*. *Porto Biomedical Journal* 6(1): e129. https://doi.org/10.1097/j.pbj.0000000000000129.

Johnson-Arbor K, Dubey R (2025). Doxorubicin. In: StatPearls [Internet]. Treasure Island (FL): StatPearls Publishing; 2025 Jan-. Available from: https://www.ncbi.nlm.nih.gov/books/NBK459232/

Jomova K, Raptova R, Alomar SY, Alwasel SH, Nepovimova E, Kuca K, Valko M (2023). Reactive oxygen species, toxicity, oxidative stress, and antioxidants: chronic diseases and aging. *Archives of Toxicology* 97(10): 2499-574. https://doi.org/10.1007/s00204-023-03562-9

Kciuk M, Gielecińska A, Mujwar S, Kołat D, Kałuzińska-Kołat Ż, Celik I, Celik I, Kontek R. (2023). Doxorubicin - An agent with multiple mechanisms of anticancer activity. *Cells* 12(4): 659. https://doi.org/10.3390/cells12040659

Kong CY, Guo Z, Song P, Zhang X, Yuan YP, Teng T, Yan L, Tang QZ (2022). Underlying the mechanisms of doxorubicin-induced acute cardiotoxicity: Oxidative stress and cell death. *International Journal of Biological Sciences* 18(2): 760-770. https://doi.org/10.7150/ijbs.65258.

Lee J, Choi MK, Song IS (2023). Recent advances in doxorubicin formulation to enhance pharmacokinetics and tumor targeting. *Pharmaceuticals (Basel)* 16(6): 802. https://doi.org/10.3390/ph16060802

Mansour DF, Hashad IM, Rady M, Abd-El Razik AN, Saleh DO (2024). Diosmin and coenzyme q10: Synergistic histopathological and functional protection against doxorubicin-induced hepatorenal injury in rats. *Toxicology Report* 13: 101848. https://doi.org/10.1016/j.toxrep.2024.101848

Mansouri E, Jangaran A, Ashtari A (2017). Protective effect of pravastatin on doxorubicin-induced hepatotoxicity. *Bratislava Medical Journal* 118: 273-277. https://doi.org/10.4149/BLL_2017_054

Mustafa S, Akbar M, Khan MA, Sunita K, Parveen S, Pawar JS, Massey S, Agarwal NR, Husain SA (2022). Plant metabolite diosmin as the therapeutic agent in human diseases. *Current Research in Pharmacology and Drug Discovery* 3: 100122. https://doi.org/10.1016/j.crphar.2022.100122

National Research Council (US) Committee for the Update of the Guide for the Care and Use of Laboratory Animals (2011). Guide for the Care and Use of Laboratory Animals. 8th ed. Washington (DC): National Academies Press (US); https://doi.org/10.17226/12910

Oliveira ML, Rocha A, Nardotto GHB, Pippa LF, Simões BP, Lanchote VL (2020). Analysis of daunorubicin and its metabolite daunorubicinol in plasma and urine with

application in the evaluation of total, renal and metabolic formation clearances in patients with acute myeloid leukemia. *Journal of Pharmaceutical & Biomedical Analysis* 191: 113576. https://doi.org/10.1016/j.jpba.2020.113576

Olorundare OE, Adeneye AA, Akinsola AO, Ajayi AM, Atolani O, Soyemi SS, Mgbehoma AI, Albrecht RM (2024). Anti-apoptotic and antioxidant mechanisms may underlie the abrogative potential of *Ocimum gratissimum* Linn. leaf extract and fractions against trastuzumab-induced cardiotoxicity in Wistar rats. *Toxicology Report* 12: 200-214. https://doi.org/10.1016/j.toxrep.2024.01.011

Owumi SE, Lewu DO, Aunsi UO, Oyelere, AK (2021). Luteolin attenuates doxorubicin-induced derangements of liver and kidney by reducing oxidative stress and inflammatory stress to suppress apoptosis. *Human & Experimental Toxicology* 40(10): 1656-72. https://doi.org/10.117/0960327121100617

Percie du Sert N, Ahluwalia A, Alam S, Avey MT, Baker M, Browne WJ, Clark A, Cuthill IC, Dirnagl U, Emerson M, Garner P, Holgate ST, Howells DW, Hurst V, Karp NA, Lazic SE, Lidster K, MacCallum CJ, Macleod M, Pearl EJ, Petersen OH, Rawle F, Reynolds P, Rooney K, Sena ES, Silberberg SD, Steckler T, Würbel H (2020). Reporting animal research: Explanation and elaboration for the ARRIVE guidelines 2.0. *PLoS Biology* 18(7): e3000411. https://doi.org/10.1371/journal.pbio.3000441

Petcu CD, Mihai OD, Tăpăloagă D, Gheorghe-Irimia RA, Pogurschi EN, Militaru M, Borda C, Ghimpețeanu OM (2023). Effects of plant-based antioxidants in animal diets and meat products: A review. *Foods* 12(6): 1334. https://doi.org/10.3390/foods12061334

Pippa LF, Oliveira ML, Rocha A, de Andrade JM, Lanchote VL (2020). Total, renal and hepatic clearances of doxorubicin and formation clearance of doxorubicinol in patients with breast cancer: Estimation of doxorubicin hepatic extraction ratio. *Journal of Pharmaceutical & Biomedical Analysis* 185: 113231. https://doi.org/10.1016/j.jpba.2020.113231

Pradubyat N, Wunnakup T, Praparatana R, Wongwiwatthananukit S, Jongrungruangchok S, Songsak T, Madaka F, Sudsai T (2024). Evaluation of antioxidant and anti-inflammatory properties, bioactive compound profiling, and molecular mechanisms of a multicomponent Thai herbal formulation. *Phytomedicine Plus* 4(4): 100662. https://doi.org/10.1016/j.phyplu.2024.100662

Pugazhendhi A, Edison TNJI, Velmurugan BK, Jacob JA, Karuppusamy I (2018). Toxicity of doxorubicin (Dox) to different experimental organ systems. *Life Science* 200: 26-30. https://doi.org/10.1016/j.lfs.2018.03.023

Punia R, Raina K, Agarwal R, Singh RP (2017). Acacetin enhances the therapeutic efficacy of doxorubicin in non-small-cell lung carcinoma cells. *PLoS ONE* 12(8): e0182870. https://doi.org/10.1371/journal.pone.0182870

Qaed E, Almaamari A, Almoiliqy M, Alyafeai E, Sultan M, Aldahmash W, Mahyoub MA, Tang Z (2024). Phosphocreatine attenuates doxorubicin-induced nephrotoxicity through inhibition of apoptosis, and restore mitochondrial function via activation of Nrf2 and PGC-1α pathways. *Chemico-Biological Interactions* 400: 111147. https://doi.org/10.1016/j.cbi.2024.111147

Rahman L, Talha Khalil A, Ahsan Shahid S, Shinwari ZK, Almarhoon ZM, Alalmaie A, Sharifi-Rad J, Calina D (2024). Diosmin: A promising phytochemical for functional foods, nutraceuticals and cancer therapy. *Food Science & Nutrition* 12(9): 6070-6092. https://doi.org/10.1002/fsn3.4271

Renu K, Pureti LP, Vellingiri B, Valsala Gopalakrishnan A (2021). Toxic effects and molecular mechanism of doxorubicin on different organs – an update. *Toxin Reviews* 41(2): 650-674. https://doi.org/10.1080/15569543.2021.1912099

Radford, J. (2024). Doxorubicin and breast cancer risk: The importance of long-term follow-up in curable cancers. *Journal of Clinical Oncology*, 42, 1868-1870. https://doi.org/10.1200/JCO.23.02763

Saleh DO, Mahmoud SS, Hassan A, Sanad EF (2022). Doxorubicin-induced hepatic toxicity in rats: Mechanistic protective role of omega-3fatty acids through Nrf2/HO-1 activation and PI3K/Akt/GSK-3β axis modulation. *Saudi Journal of Biological Sciences* 20(7): 103308. https://doi.org/10.1016/j.sjbs.2022.103308

Song S, Chu L, Liang H, Chen J, Liang J, Huang Z, Zhang B, Chen X (2019). Protective effects of dioscin against doxorubicin-induced hepatotoxicity via regulation of Sirt1/FOXO1/NF-κb signal. *Frontiers in Pharmacology* 10: 1030. https://doi.org/10.3389/fphar.2019.01030

Tammam AA-E, Khalaf AAA, Zaki AR, Khalifa MM, Ibrahim MA, Mekkawy AM, Abdelrahman R, Farghali AA, Noshy P (2022). Hesperidin protects rats' liver and kidney from oxidative damage and physiological disruption induced by nickel oxide nanoparticles. *Frontiers in*

Physiology 13: 912625. https://doi.org/10.3389/fphys.2022.912625

Ullah A, Munir S, Badshah SL, Khan N, Ghani L, Poulson BG, Emwas AH, Jaremko M (2020). Important flavonoids and their role as a therapeutic agent. *Molecules* 25(22): 5243. https://doi.org/10.3390/molecules25225243

van der Zanden S Y, Qiao X, Neefjes J (2021). New insights into the activities and toxicities of the old anticancer drug doxorubicin. *FASEB Journal* 288(21): 6079-304. https://doi.org/10.1111/febs.15583

Xiang C, Yan Y, Zhang D (2021). Alleviation of the doxorubicin-induced nephrotoxicity by fasudil *in vivo* and *in vitro*. *Journal of Pharmacological Sciences* 145(1): 6-15. https://doi.org/10.1016/j.jphs.2020.10.002 Yang N, Ma H, Jiang Z, Niu L, Zhang X, Liu Y, Wang Y, Cheng S, Deng Y, Qi H, Wang Z. (2019). Dosing depending on SIRT3 activity attenuates doxorubicin-induced cardiotoxicity via elevated tolerance against mitochondrial dysfunction and oxidative stress. *Biochemical & Biophysical Research Communications* 517(1): 111-117. https://doi.org/10.1016/j.bbrc.2019.07.029.